

BUBBLE FORMATION AT AN ORIFICE IN AN INVISCID LIQUID

By J. F. DAVIDSON, M.A., Ph.D., A.M.I.Mech.E.* and B. O. G. SCHÜLER, Ph.D.*

SUMMARY

The periodic formation of bubbles due to the flow of gas into an inviscid liquid has been studied both experimentally and theoretically. Two systems were studied:

(i) The simplest case is when gas flows through an orifice into the liquid at a constant volumetric rate, so that the movement and growth of the bubble do not influence the gas flow rate. In this case a simple theory, based on first principles, gives a rough estimate of the relation between bubble volume and flow rate.

(ii) When gas passes into the forming bubble from an infinite vessel at constant pressure, the theory has to be modified to allow for the change in gas flow rate into the bubble as it forms. Nevertheless, the relation between gas flow rate, \bar{C} , and bubble volume \bar{V} is similar to the relation for case (i). However, when the pressure in the vessel is reduced, \bar{C} and \bar{V} are suddenly reduced to zero at a certain value of the vessel pressure, so that there are critical values of \bar{C} and \bar{V} . These critical values of pressure, flow, and bubble volume are in rough agreement with experimental values, and it is hoped that this theory will throw some light on the phenomenon of "dumping" on sieve plates.

Introduction

This paper describes an experimental and theoretical investigation of the formation of gas bubbles at an orifice in an inviscid liquid. The main purpose of the paper is to describe a theory of bubble formation by means of which the size and frequency of bubbles can be calculated. This attempt has been only partly successful in that the size and frequency of the bubbles do not always agree with experiment, but the theory is nevertheless valuable in assessing the approximate effect of the various parameters. In particular, the theory is valuable in predicting that there is a critical gas flow rate for continuous bubble formation in the so-called "constant pressure" experiments. In these experiments, air was passed through a single hole of radius r_0 in a horizontal plate into a finite depth of liquid above the plate. It is clear that for bubbles to form, the pressure P_1 in the vessel below the plate must exceed a minimum value equal to the sum of the static head of liquid h above the plate plus a surface tension term $2\sigma/r_0$. The theory shows—and experiments confirm—that if the vessel below the orifice plate is large, then as soon as P_1 is greater than $\rho gh + 2\sigma/r_0$, bubbles of a finite size will form continuously, so that the gas flow rate suddenly increases from zero to a finite amount. Here ρ is the liquid density and g the acceleration of gravity. This finite gas flow is of the same order of magnitude as the critical gas flow per hole on a sieve plate, the so-called "dumping rate".^{1, 2}

The paper also deals with studies of bubble formation with a constant gas flow rate, the constant flow being obtained by feeding the air into the liquid through a restriction such as a capillary or sinter, so that there is a large pressure drop between the gas reservoir and the feed to the bubble. This arrangement is of less practical importance, but is simpler to treat theoretically and is therefore useful in assessing the merits of the theory.

The present work is a continuation of work described in a previous paper on bubble formation in a viscous liquid.³

Numerous investigators⁴⁻¹⁶ have measured the volume of bubbles formed when air or other gas is blown into an inviscid liquid. These experiments fall into three classes:

* University of Cambridge, Department of Chemical Engineering, Pembroke St., Cambridge.

(i) With a very low gas rate^{4, 5, 6, 7, 8} the mechanism of bubble formation is similar to the mechanism of drop formation in the "drop weight" method of determining surface tension. These gas flow rates are much less than those considered in the present paper.

(ii) When the bubbles were formed at the end of a tube a few millimetres in diameter^{9, 10, 11} or at an orifice connected to a small gas buffer vessel, the conditions approached those of constant gas flow during bubble formation.

(iii) Where the gas buffer vessel was larger,¹²⁻¹⁶ the conditions were more nearly those of constant pressure, though with an intermediate sized vessel, the volume of the vessel is an important factor determining bubble size.

No previous attempts appear to have been made to predict bubble volumes and frequencies from theory, though Hayes, Hardy, and Holland¹⁶ have written down equations describing the vertical motion of the bubble during formation.

Experimental

Apparatus for bubble formation

The apparatus has been described in detail in a previous paper.³ The liquid in which bubbles were formed was contained in a vertical tube of 14.7 cm internal diameter with liquid depths up to 15 cm. This tube was mounted with its axis vertical, on top of a 45-litre drum which acted as a buffer, gas being fed steadily into the drum and passing out as bubbles through an orifice at the base of the cylinder containing the liquid. Orifices of three kinds were used, and are illustrated in Fig. 2 of the previous paper:³

(a) For the constant pressure experiments, the orifice was essentially a plain hole in a horizontal plate with a diameter between 0.29 and 0.46 cm.

(b) For the constant flow experiments with large gas flow rates, the orifice consisted of two plates. The top plate was in contact with the liquid and was drilled with a plain hole with a diameter between 0.30 cm and 0.50 cm. The bubbles formed immediately above this hole, and to ensure constant flow a sintered plate was brazed on below the hole.

(c) For the constant flow experiments with smaller flow rates, the gas was passed into the liquid through a long capillary. The end of the capillary where the bubbles formed was let into a horizontal plate so that the bubbles were formed under conditions similar to those with orifices (a) and (b) above.

The arrangements for measuring gas flow and drum pressure were described previously.³

In most of the experiments the bubble frequency was measured by a stroboscope. In some of the constant pressure experiments, the bubble-formation was not regular enough for the use of a stroboscope, and it was necessary to take ciné photographs to measure the volumes of the individual bubbles. For this purpose a Pathe Webó ciné camera was available, with up to 80 frame/s, and a minimum exposure time of about 1/600 s.

Constant Flow

Theory

The assumptions used in deriving the theory are similar to those described in the previous paper:³ the bubble is assumed to be spherical at all times during formation, and the upward motion is determined by a balance between the buoyancy force and the upward mass acceleration of the fluid surrounding the bubble. Thus the equation of upward motion is:

$$Vg = \frac{d}{dt} \left(\frac{11}{16} V \frac{ds}{dt} \right) \quad (1)$$

V being the volume of the bubble at time t after it started growing, and s the vertical distance of the centre of the bubble above the point where the gas enters the liquid.

The assumptions and terms neglected in deriving equation (1) are:

(i) The flow around the bubble is assumed to be irrotational and unseparated, and the effective inertia of the surrounding fluid has been taken as $11\rho V/16$.³ Because of this assumption, the drag coefficient is zero. Hayes, Hardy, and Holland¹⁶ assigned a drag coefficient to a forming bubble, thereby assuming that there is a fully established wake behind each bubble as it forms. However, when a solid sphere or cylinder is accelerated from rest in a fluid, the initial motion is practically irrotational, and the wake is not fully established until the body has moved an appreciable distance.^{17, 18} It seems likely that the flow round the accelerating bubble will be similar, and consequently the drag coefficient is likely to be negligible until after the bubble has detached from the orifice.

(ii) Neglect of the upward momentum of the gas leaving the orifice is justified by calculations previously described.³

With a constant gas flow G , and an initial bubble volume of zero, $V = Gt$; by substituting this relation in equation (1), the latter can be integrated. When $t = 0$, $ds/dt = 0$, and assuming that the bubble growth is terminated when its radius r equals s the distance travelled, gives the final bubble volume³

$$V_1 = 1.378 \frac{G^{6/5}}{g^{3/5}} \quad (2)$$

As each bubble breaks away from the orifice it leaves behind a volume of gas V_0 which forms a nucleus for the next bubble. In the derivation of equation (2) it was assumed that V_0 was much less than V_1 , but with larger orifices V_0 is not negligible and it is necessary to put

$$V = \frac{4}{3} \pi r^3 = Gt + V_0 \quad (3)$$

when integrating equation (1). This gives, with the initial conditions $s = ds/dt = 0$,

$$s = \frac{16g}{11} \left[\frac{t^2}{4} + \frac{V_0 t}{2G} - \frac{V_0^2}{2G^2} \ln \left(\frac{Gt + V_0}{V_0} \right) \right] \quad (4)$$

The bubble is assumed to detach when $s = r + r_0$, and the lifetime of the bubble is obtained by plotting equation (4), and plotting $r + r_0$ as a function of time from equation (3) on the same axes. Here r_0 is the radius of the orifice supplying the gas and it is assumed that $V_0 = 4\pi r_0^3/3$.

Experimental results

The results are classified according to the flow rate; when this is small, equation (2) is appropriate, and equations (3) and (4) are used for larger flow rates.

Fig. 1 shows the results for small flow rates compared with equation (2). It will be seen that above a flow rate of 1.5 ml/s the results are in excellent agreement with theory. At the lower flows the discrepancy between theory and experiment is greatest for the larger orifice with air bubbling into water. Approximate calculations suggested that the discrepancy is

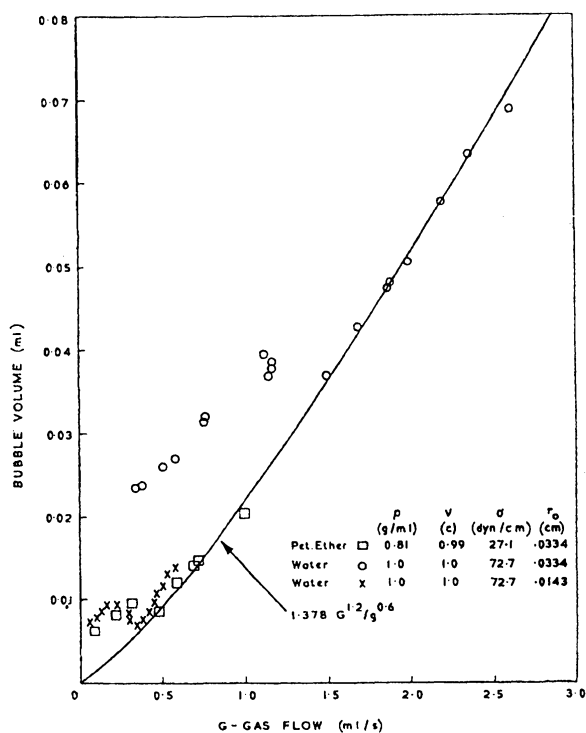


Fig. 1.—Experimental and theoretical bubble volumes for small constant flow rates

due to the influence of surface tension acting round the rim of the orifice, as it does in "drop weight" experiments, and of course as the flow rate tends to zero the bubble volume is determined by the balance between surface tension and buoyancy forces, as in the "drop weight" method.

Fig. 2 shows the results for higher flow rates, compared with theoretical curves calculated from equations (3) and (4) using various values of r_0 . These theoretical curves give bubble volumes that are somewhat higher than those given by equation (2). With these higher flow rates, the double and quadruple bubble formation observed by Helsby and Tuson¹⁹ was seen to occur. This made the stroboscopic method impracticable, and to measure the bubble volume it was necessary to

$$1.378 = \frac{1}{4} \left(\frac{12}{\pi} \right)^{1/5} 11^{3/5}$$

take ciné pictures of the forming bubbles. The volume of each individual bubble could be calculated from the pictures, and for comparison with theory Fig. 2 shows the volume of the leading bubble in the series of two or four, before coalescence.

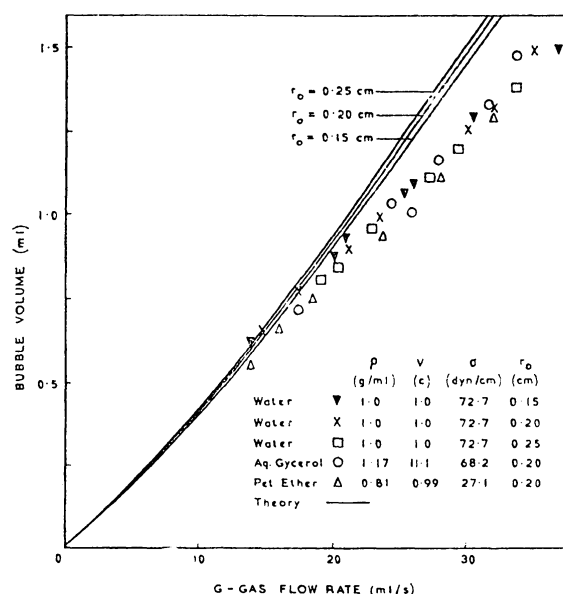


Fig. 2.—Experimental and theoretical bubble volumes for large constant flow rates

Fig. 3 shows bubble formation in groups of two. It will be seen that the forming bubble is roughly spherical, and that each bubble does not assume the spherical cap shape, characteristic of fully separated flow,²⁰ until it has moved some distance from the orifice. These photographs therefore justify, to some extent, the assumption of unseparated flow during formation.

Fig. 2 shows good agreement between theory and experiment for flows between 15 and 20 ml/s, as in the range 1.5–3 ml/s shown in Fig. 1. Data were not taken for the intermediate

range 3.0–15 ml/s but there is good reason to suppose that theory and experiment would agree in this range. At flow rates above 20 ml/s the divergence between theory and experiment is believed to be partly due to the upward current induced by the bubbles in the liquid surrounding the orifice and partly due to the deformation of the forming bubbles from the spherical shape. Because of the upward current, each forming bubble is dragged upwards and therefore has a smaller volume than the theoretical bubble which is imagined to form in a stagnant liquid. Also, the flattening of the base of the forming bubbles may cause them to detach earlier than the idealized spherical bubbles.

Constant Pressure

Theory

The upward motion of the forming bubble is determined by equation (1) in the same way as for the theory of the constant flow experiment. As in the previous paper,³ it is supposed that gas flows into the bubble, from a vessel at constant pressure, through an orifice whose characteristic constant k is determined by an experiment in which the gas under consideration flows steadily through the orifice in the absence of liquid. The orifice is such that the volume flow rate of gas is k times the square root of the pressure difference across the orifice, and when the bubble is forming, the flow rate is given by:

$$\frac{dV}{dt} = k \left[P + \rho g s - \frac{2\sigma}{r} \right]^{1/2} \quad (5)$$

Here $P = P_1 - \rho g h$. Equations (1) and (5) were solved numerically by the computer Edsac 2, with the initial conditions at $t = 0$:

$$s = 0, \frac{ds}{dt} = 0, V_0 = \frac{4}{3} \pi r_0^3.$$

The bubble was assumed to detach when $s = r + r_0$, and the results are plotted in the form of dimensionless groups in Figs 4, 5, and 6. The dimensionless groups were formulated from equations (1) and (5) with σ and $r_0 = 0$, when there are unique relations between the dimensionless bubble volume $V' = V/\rho^{3/4} k^{3/2}$, the dimensionless pressure $P' = P/gk^{1/2} \rho^{5/4}$,

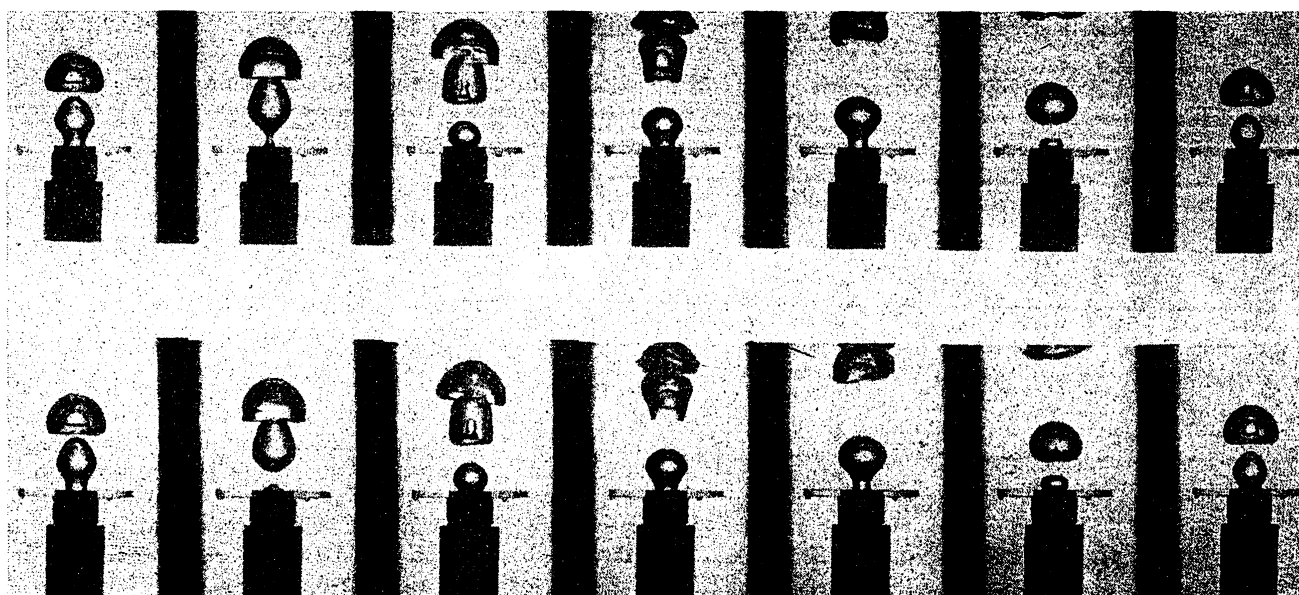


Fig. 3.—Bubble formation in groups of two with a constant flow rate of 13.7 ml/s. $r_o = 0.2$ cm

and the dimensionless flow $G' = \bar{G}/k^{5/4}g^{1/2}\rho^{5/8}$. Here $\bar{V} = V_1 - V_0$, and \bar{G} is the mean flow rate during bubble formation, and is \bar{V}/t_1 , where t_1 is the time at detachment. For the case when $\sigma = 0$ and $r_0 = 0$, these variables are related

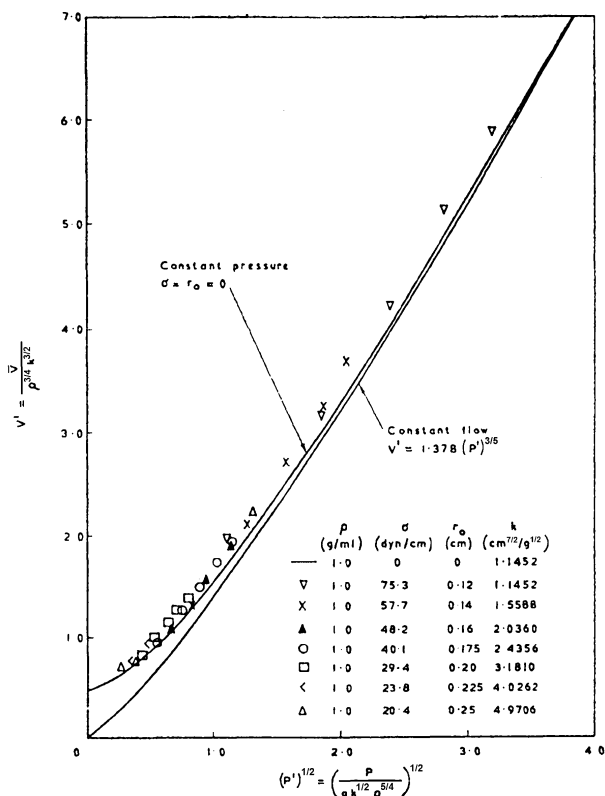


Fig. 4.—The theoretical relations between dimensionless bubble volume and pressure. When $P' = 0$, $V' = 0.500$ for constant pressure. The points as well as the curves were derived from theory

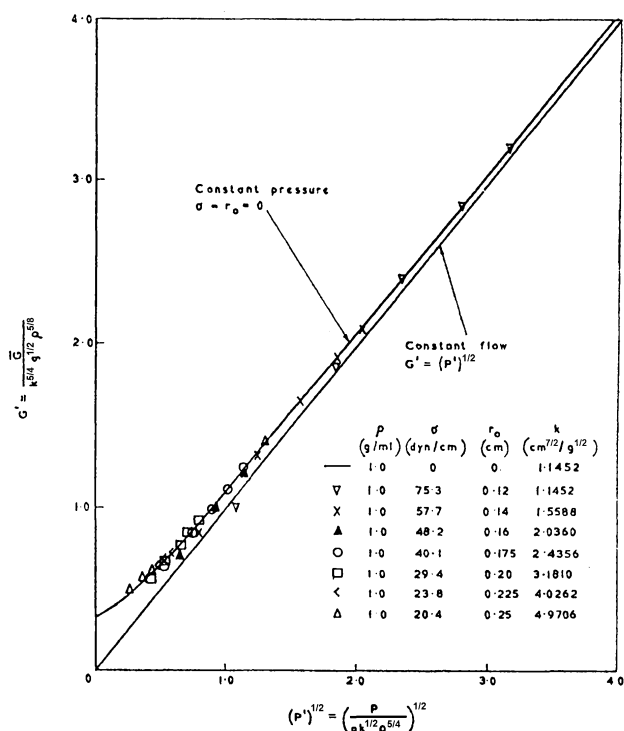


Fig. 5.—The theoretical relations between dimensionless flow rate and pressure. When $P' = 0$, $G' = 0.351$ for constant pressure. The points as well as the curves were derived from theory

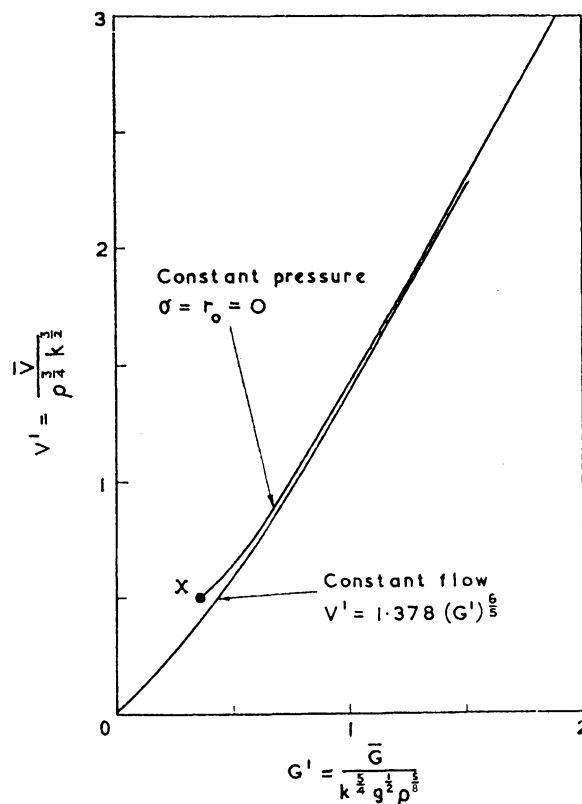


Fig. 6.—The theoretical relations between dimensionless bubble volume and flow rate. At the point X, $V' = 0.500$, $G' = 0.351$

by the curves shown in Figs 4, 5, and 6, and the diagrams also show results for various values of σ and r_0 . It is apparent that the effect of σ and r_0 upon bubble volume and mean gas flow rate is small. Surface tension does however affect the minimum value of P for bubbling to occur, since bubbling will cease if P is less than $2\sigma/r_0$. It should also be noted that of Figs 4, 5, and 6, only two are independent, and the third can be plotted from the other two. In most practical problems the gas flow rate is fixed beforehand, and the bubble volume \bar{V} and the pressure P have to be determined.

The significance of the diagrams can be better understood by considering two limiting cases as follows:

k SMALL; APPROACH TO CONSTANT FLOW

When the orifice constant k is very small, P will become large for any flow to pass, and the flow will not vary during bubble formation. Substituting $G = kP^{1/2}$ in equation (2) it is easily shown that $V' = 1.378 (P')^{3/5}$, $G' = (P')^{1/2}$, and these relations are shown plotted on Figs 4, 5, and 6, and, as would be expected, they approach the "constant pressure" curves asymptotically.

In Fig. 5, the horizontal distance between the "constant pressure" curve and the "constant flow" line is a measure of the difference between the actual pressure drop through the system and the pressure drop which would be obtained if the flow through the orifice were uniform and equal to \bar{G} . This means that the normal method of calculating pressure drops through bubbling devices by adding together a static liquid head, a surface tension term, and a hole pressure-drop term gives a total pressure drop which is too high, since all these pressure drops do not act simultaneously.

$P = 0$; THE CRITICAL FLOW

The "constant pressure" curves in Figs 4 and 5 show that when $P = 0$, \bar{G} and \bar{V} have finite values. This discontinuity is due to the presence in equation (5) of the term $\rho g s$, which gives a finite pressure difference across the orifice as soon as the bubble starts to move. With a finite value of the surface tension, the minimum value of P is $2\sigma/r_0$, and if \bar{V} is plotted as a function of P , the curve will show a step up, at $P = 2\sigma/r_0$, from zero to the value of \bar{V} given by Fig. 4.

With $\sigma = 0$ and $P = 0$, equation (5) becomes

$$dV/dt = k(\rho g s)^{1/2},$$

and this equation together with equation (1) has the following analytical solution for $r_0 = 0$:

$$V = \left(\frac{2\rho}{33}\right)^{1/2} k g t^2 \quad s = \frac{8}{33} g t^2 \quad (6)$$

The bubble will detach when $s = (3V/4\pi)^{1/3}$, giving the volume \bar{V} of the detached bubble and the mean flow rate \bar{G} as follows:

$$V' = \frac{\bar{V}}{k^{3/2}\rho^{3/4}} = \left(\frac{33}{32}\right)^{3/4} \left(\frac{3}{4\pi}\right)^{1/2} = 0.500, \quad (7)$$

$$G' = \frac{\bar{G}}{k^{5/4}g^{1/2}\rho^{5/8}} = \frac{2^{1/2}}{4} \left(\frac{33}{2}\right)^{1/8} \left(\frac{3}{4\pi}\right)^{1/4} = 0.351. \quad (8)$$

These numbers agree well with the values calculated from the computer results.

Experimental results

Experimental results with the "constant pressure" arrangement are shown in Table I, and Figs 7, 8, and 9 show the results graphically for $r_0 = 0.149$ cm. These results show clearly the phenomenon of the critical pressure, with a sudden rise in bubble volume and mean flow rate when P is nearly $2\sigma/r_0$. Comparing Figs 7 and 8, it can be seen that when \bar{G} is reduced below its critical value (about 32 ml/s), \bar{V} changes

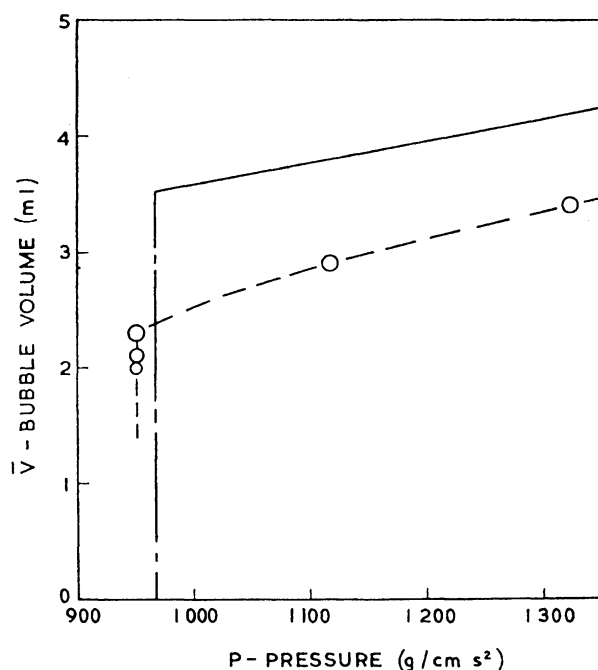


Fig. 7.—Bubble volume as a function of pressure with air and water. $k = 1.90$, $r_0 = 0.149$ cm

very little, and this is in accordance with the theory which predicts that \bar{V} should stay constant when \bar{G} is less than its critical value. For this reason, the theoretical line on Fig. 7 is shown chain dotted, since when $P = 968$, \bar{V} can be either zero or 3.5. But in Fig. 8, the theoretical line is shown continuous, because at $P = 968$, all values of \bar{G} between 0 and 67 are possible. Intermediate values of \bar{G} between 0 and 67 give a bubble volume of 3.5 ml. Figs 7 and 8 show that when P is greater than 968 the theoretical flow rate and bubble volume are considerably greater than the experimental values, and the differences are thought to be due partly to the upward current of water caused by the stream of rising bubbles, and partly due to bubble deformation; these two factors were discussed in connection with constant flow results shown in Fig. 2.

Fig. 9 shows bubble volume \bar{V} plotted as a function of mean flow \bar{G} . When \bar{G} is less than 67, the theoretical value of

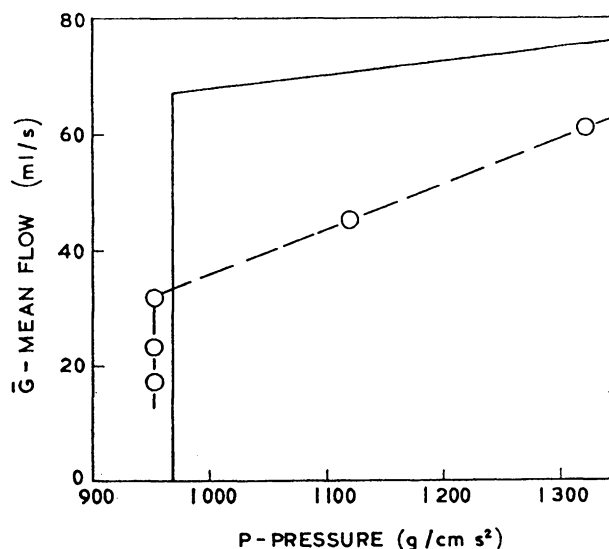


Fig. 8.—Mean flow rate as a function of pressure, with air and water. $k = 1.90$, $r_0 = 0.149$ cm

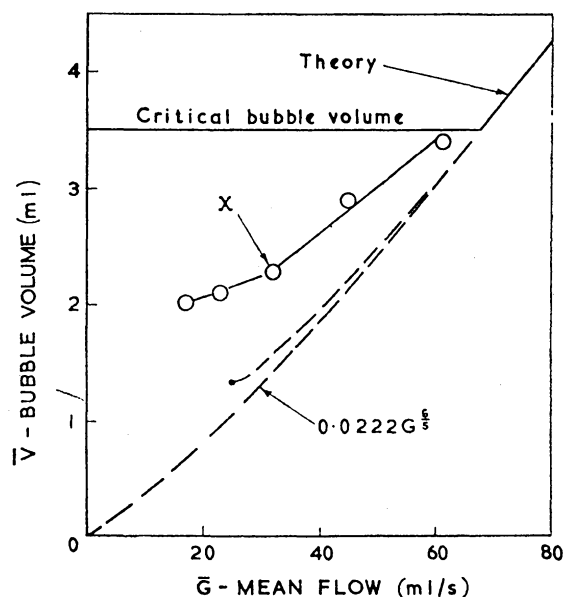


Fig. 9.—Bubble volume as a function of mean flow for constant pressure with air and water. $k = 1.90$, $r_0 = 0.149$ cm. X is the experimental point of critical pressure

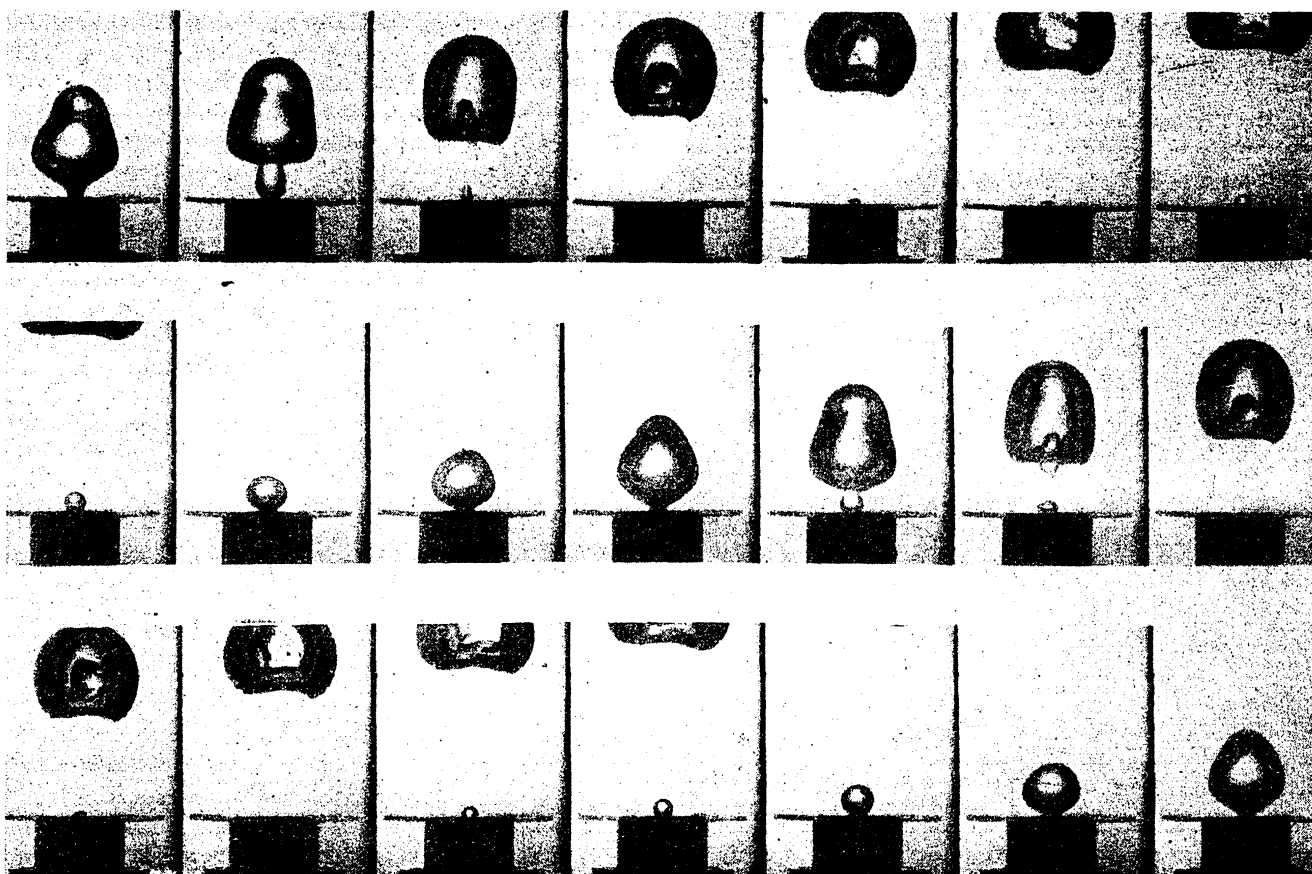


Fig. 10.—Bubble formation at constant pressure with a mean flow rate below the critical value. $\bar{G} = 26 \text{ ml/s}$, $k = 3.06 \text{ ml cm}^{1/2}/\text{g}^{1/2}$, $r_0 = 0.187 \text{ cm}$

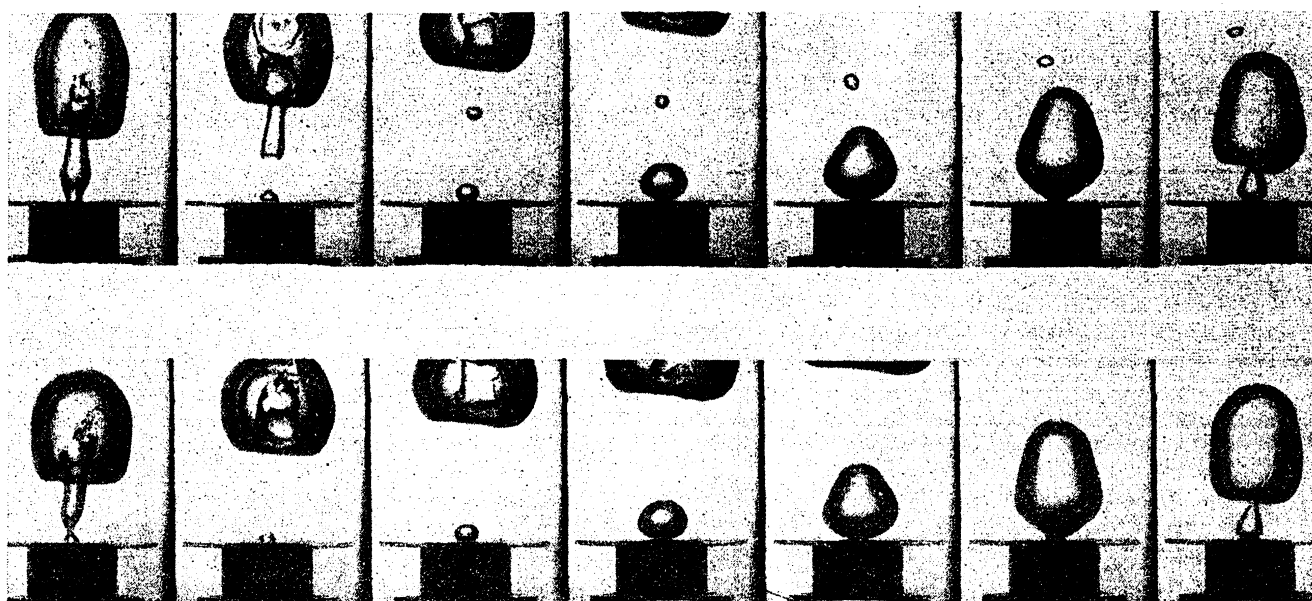


Fig. 11.—Bubble formation at constant pressure with a mean flow rate above the critical value. $\bar{G} = 60 \text{ ml/s}$, $k = 3.06 \text{ ml cm}^{1/2}/\text{g}^{1/2}$, $r_0 = 0.187 \text{ cm}$

\bar{V} is constant at 3.5, and the dotted curves are merely continuations of the theoretical curves for "constant pressure" and "constant volume". At a given value of P , the experimental values of \bar{V} and \bar{G} are both less than the theoretical, and consequently the points on Fig. 9 are shifted down towards the bottom left hand corner of the diagram, and this shift includes the critical flow point X. In design work, \bar{G} is the independent

variable, and Fig. 9 shows that for low values of \bar{G} , the actual value of \bar{V} is less than the theoretical, but for high values of \bar{G} the simple formula from the "constant volume" theory gives an approximate representation of the actual bubble volumes. Table 1 shows that the characteristics of Figs 7, 8, and 9 are accentuated for the larger orifices

In comparing "constant flow" and "constant pressure"

TABLE I.—Formation of Air Bubbles in Water with Constant Gas Pressure
 $\sigma = 72 \text{ dyn/cm}$

k (ml cm ^{1/2} /g ^{1/2})	r_0 (cm)	$\frac{2\sigma}{r_0}$ (g/cm s ²)	P (g/cm s ²)	Mean flow \bar{G}		Bubble volume \bar{V}		
				Expt. (ml/s)	Theory (ml/s)	Expt. (ml)	Theory (ml)	$0.0222 \bar{G}_{\text{expt}}^{6/5}$
1.90	0.149	968	951	17	67	2.0	3.5	0.67
1.90	0.149	968	951	23	67	2.1	3.5	0.96
1.90	0.149	968	951	32	67	2.3	3.5	1.42
1.90	0.149	968	1118	45	70	2.9	3.8	2.14
1.90	0.149	968	1323	61	76	3.4	4.2	3.06
3.06	0.187	771	779	26	102	3.2	6.1	1.11
3.06	0.187	771	779	33	102	3.4	6.1	1.48
3.06	0.187	771	877	47	105	4.1	6.4	2.26
3.06	0.187	771	1024	60	112	4.5	6.9	3.04
3.82	0.206	698	734	17	124	4.1	7.8	0.67
3.82	0.206	698	734	30	124	4.3	7.8	1.31
3.82	0.206	698	832	57	129	4.9	8.3	2.84
3.82	0.206	698	1006	68	141	5.7	9.1	3.53
4.90	0.230	625	632	25	156	5.6	10.7	1.06
4.90	0.230	625	739	60	163	6.9	11.4	3.04
4.90	0.230	625	790	68	169	7.1	11.7	3.53
4.90	0.230	625	800	70	169	7.5	11.8	3.64

experiments (Figs 2 and 9), it should be noted that in the latter experiments the effect of the "neck" formed during detachment will be more important, because in the one case \bar{V} is proportional to t and in the other case to t^2 . This means that the bubble formed in the "constant pressure" experiment will receive a greater proportion of its gas during the detachment period. Figs 10 and 11, which are ciné pictures of bubbles forming in a "constant pressure" experiment, do show the very great rate of bubble expansion during detachment, compared with the "constant flow" bubbles shown in Fig. 3.

Figs 10 and 11 also demonstrate bubble formation with pressures above and below the critical. Fig. 10 shows that, below the critical pressure, there is a discrete time interval between one bubble and the next—the magnitude of the interval depending upon the size of the gas reservoir below the orifice—whereas Fig. 11 shows continuous bubble formation.

Conclusions

Experiments with a constant gas flow rate during bubble formation have shown that equation (2) can be used as a rough guide to the relation between the bubble volume \bar{V} and the gas flow rate \bar{G} . This equation can also be used when the bubbles form above an orifice with a constant supply pressure below, provided the gas flow rate is somewhat above the critical flow rate.

If the gas flow rate is less than or equal to this critical flow rate, the bubble size will be roughly constant, and the time interval between the bubbles will depend upon the volume of the vessel below the orifice. If this vessel is infinitely large, bubble formation will cease altogether when the pressure P is less than $2\sigma/r_0$.

It seems likely that the critical flow rate described in the present paper is closely related to the flow rate at which downward leakage or "dumping" will occur on a sieve plate, because if the total gas flow divided by the number of holes is less than the critical value of \bar{G} , some of the holes will not be bubbling continuously, and the opportunity for leakage will occur.

Acknowledgment

The authors wish to acknowledge the help of Mr. H. P. F. Swinnerton-Dyer, who programmed the calculations for Edsac 2. One of us (J. F. D.) wishes to acknowledge the support of the University of Delaware during the time when this paper was written.

Symbols Used

- G = constant gas flow rate.
- \bar{G} = mean flow rate in "constant pressure" experiment
= \bar{V}/t_1 .
- $G' = \bar{G}/k^{5/4}g^{1/2}\rho^{5/8}$.
- g = acceleration due to gravity.
- h = depth of liquid seal.
- k = orifice constant = (flow rate)/(pressure difference)^{1/2}.
- $P = P_1 - \rho gh$.
- P_1 = pressure in the vessel below the orifice.
- $P' = P/g k^{1/2}\rho^{5/4}$.
- r = radius of bubble at any instant.
- r_0 = radius of orifice.
- s = vertical distance moved by the bubble.
- t = time.
- t_1 = time at detachment.
- \bar{V} = bubble volume at time t .
- $V_0 = 4\pi r_0^3/3$.
- V_1 = bubble volume just before detachment.
- $\bar{V} = V_1 - V_0$.
- $V' = \bar{V}/\rho^{3/4}k^{3/2}$.
- ρ = liquid density.
- σ = surface tension.

The above quantities may be expressed in any set of consistent units in which force and mass are not defined independently.

References

- ¹ Mayfield, F. D., Church, W. L., Green, A. C., Lee, D. C. and Rasmussen, R. W. *Ind. Engng Chem.*, 1952, **44**, 2238.
- ² Brown, R. S. *Ph.D. Thesis*, Lawrence Radiation Laboratory, Berkeley, California, 1958.
- ³ Schüler, B. O. G. and Davidson, J. F. *Trans. Instn chem. Engrs*, 1960, **38**, 144.
- ⁴ Guyer, A. and Peterhans, F. *Helv. Chim. Acta.*, 1943, **26**, 1099.
- ⁵ Datta, R. L., Napier, D. H., and Newitt, D. M. *Trans. Instn chem. Engrs*, 1950, **28**, 14.
- ⁶ Van Krevelen, D. W. and Hoftijzer, P. J. *Chem. Engng Progr.*, 1950, **46**, 29.
- ⁷ Coppock, P. D. and Meiklejohn, G. T. *Trans. Instn chem. Engrs*, 1951, **29**, 75.
- ⁸ Benzinger, R. J. and Myers, J. E. *Industr. Engng Chem.*, 1955, **47**, 2087.
- ⁹ Eversole, W. G., Wagner, G. H. and Stackhouse, E. *Industr. Engng Chem.*, 1941, **33**, 1459.
- ¹⁰ Calderbank, P. H. *Trans. Instn chem. Engrs*, 1956, **34**, 70.

- ¹¹ Siemes, W. and Kaufmann, J. F. *Chemical Engineering Science*, 1956, 5, 127.
- ¹² Hughes, R. R., Handlos, A. M., Evans, H. D. and Maycock, R. L. *Publication of the Heat Transfer and Fluid Mechanics Institute, Los Angeles*, 1953.
- ¹³ Quigley, C. J., Johnson, A. I. and Harris, B. L. *Chemical Engineering Progress Symposium Series No. 16*, 1955, 31.
- ¹⁴ Davidson, L. and Amick, E. H. *A.I.Ch.E. Journal*, 1956, 2, 337.
- ¹⁵ Leibson, I., Holcomb, E. G., Cacosso, A. G. and Jacmic, J. J. *A.I.Ch.E. Journal*, 1956, 2, 296.
- ¹⁶ Hayes, W. B., Hardy, D. W., and Holland, C. D. *A.I.Ch.E. Journal*, 1959, 5, 319.
- ¹⁷ Prandtl, L. and Tietjens, O. G. "*Applied Hydro- and Aeromechanics*", 1934, (New York : McGraw-Hill Book Co.).
- ¹⁸ Goldstein, S., "*Modern Developments in Fluid Dynamics*," 1938 (Oxford: The University Press).
- ¹⁹ Helsby, F. W. and Tuson, K. R. *Research*, 1955, 8, 270.
- ²⁰ Davies, R. M. and Taylor, G. I. *Proc. Roy. Soc.*, 1950, A200, 375.

The manuscript of this paper was received on 26 May, 1960 and the paper was presented at a symposium of the Institution in London on 10 October, 1960.